https://doi.org/10.5194/tc-2020-32
Preprint. Discussion started: 4 March 2020

The Cryosphere Discussions

Geothermal flux beneath the Antarctic Ice Sheet derived from measured temperature profiles in deep boreholes

Pavel Talalay[1], Yazhou Li[1], Laurent Augustin[2], Gary D. Clow[3,4], Jialin Hong[1], Eric Lefebvre[5], Alexey Markov[1], Hideaki Matoyama[6], Catherine Ritz[5]

[1]Polar Research Center, Jilin University, 130021 Changchun, China
[2]Division Technique de l'INSU, CNRS, 83507 La Seyne sur Mer, France
[3]Geosciences and Environmental Change Science Center, U.S. Geological Survey, Lakewood, Colorado, USA
[4]Institute of Arctic and Alpine Research, University of Colorado Boulder, Boulder, Colorado, USA
[5]Université Grenoble Alpes, CNRS, IRD, IGE, 38000 Grenoble, France
[6]National Institute of Polar Research, Tokyo, Japan

Correspondence to: Pavel Talalay (ptalalay@yahoo.com)

Abstract. The temperature at the Antarctic ice sheet bed and the temperature gradient in subglacial rocks have been directly measured only a few times, although extensive thermodynamic modelling has been used to estimate geothermal heat flux under ice sheet. During the last five decades, deep ice-core drilling projects at six sites – Byrd, WAIS Divide, Dome C, Kohnen, Dome F, and Vostok – have succeeded in reaching to, or nearly to, the bed in inland locations in Antarctica. When temperature profiles in these boreholes and heat flow model are combined with estimations of vertical velocity, the heat flow at ice sheet base is translated to a geothermal heat flux of 117.8±3.3 mW m^{-2} at Byrd, 67.3±8.6 mW m^{-2} at Dome C, 79.0±5.0 mW m^{-2} at Dome F, and -3.3±5.6 mW m^{-2} at Vostok, close to predicted values. However, estimations at Kohnen and WAIS Divide gave flux of 161.5±10.2 mW m^{-2} and 251.3±24.1 mW m^{-2}, respectively, far higher than that predicted by existing heat flow models. The question arises as to whether this high heat flow represents regional values, or if the Kohnen and WAIS Divide boreholes were drilled over local hot spots.

1 Introduction

Geothermal heat flux (GHF) is one of the key drivers of basal melt in Antarctica and thus is one of the primary issues impacting the role of the cryosphere on the sea level, via the past, present and future contribution of land ice to sea level change. The average global surface GHF is ~86 mW m^{-2}, which varies from 64.7 mW m^{-2}, the mean continental heat flow (including arcs and continental margins), to 95.9 mW m^{-2}, the mean oceanic heat flow (Davies, 2013). However, several geological factors including heat from the mantle, heat production in the crust by radioactive decay, and tectonic history, cause spatially variable GHF in Antarctica.

Most studies of GHF in Antarctica rely on thermal models (Pattyn, 2010; Van Liefferinge and Pattyn, 2013). Modeling studies on the base of a global seismic survey and the structural similarity of crust and upper mantle showed that the Western Antarctic Ice Sheet (WAIS) has a GHF three times higher than that of the East Antarctic ice sheet (EAIS) (Shapiro and

https://doi.org/10.5194/tc-2020-32
Preprint. Discussion started: 4 March 2020

Ritzwoller, 2004). For a central point in the WAIS (78S, 110W), the average GHF is expected to be 110 mW m^{-2}. The GHF can also be estimated on the basis of geological information, where uniform values are attributed to large geologically homogeneous areas (An et al., 2015; Goodge, 2018; Llubes et al., 2006; Martos et al., 2015; Pollard et al., 2005).

Some studies suggest using remote methods to estimate GHF underneath the Antarctic ice sheet. For example, satellite magnetic data showed that the GHF underneath the ice sheet varies from 40 to 185 mW m^{-2} and that areas of high GHF coincide with known current volcanism and some areas known to have ice streams (Fox Maule et al., 2005). In the central part of the EAIS, the average GHF was estimated to be in the range of 50 to 60 mW m^{-2}; however, elevated GHFs were found along the WAIS–EAIS boundary and around the Siple Coast. Similarly, high GHFs were found around Victoria Land, Oates Land, and George V Land. Observations of crustal heat production within the continental crust underneath the Lambert-Amery glacial system in East Antarctica also show high heat flux of at least 120 mW m^{-2} (Pittard et al., 2016).

Direct temperature measurement obviously produces the most reliable GHF estimations and can be used to verify results of preliminary thermal modeling and geological-geophysical studies. While over 10,000 heat flow measurements have been made globally, 90% are from Europe, North America, and southern Africa. South America, Asia and Australia have far fewer measurements, and Antarctica has virtually none (Neumann et al., 2000). Because drilling through the thick ice is extremely complicated, time-consuming, and expensive, direct temperature measurements in Antarctic subglacial till/bedrock environments have only been conducted twice so far, both under the WAIS: at the subglacial Lake Whillans (285±80 mW m^{-2}) (Fisher et al., 2015) and near the grounding zone of the Whillans Ice Stream (88±7 mW m^{-2}) (Begeman et al., 2017), ~100 km apart (Fig. 1). The tremendous difference between these two adjacent sites suggests a high spatial variability of GHF.

More reliable GHF estimations under the Antarctic ice sheet can be made from available temperature profiles in ice boreholes. During the last five decades, deep ice-core drilling projects at six sites – Byrd (Ueda and Garfield, 1970), WAIS Divide (Slawny et al., 2014), Dome C (Augustin et al., 2007), Kohnen (Wilhelms et al., 2014), Dome F (Motoyama, 2007), and Vostok (Lukin and Vasiliev, 2014; Vasiliev et al., 2011) – have succeeded in reaching, or nearly reaching, the ice sheet bed at inland locations in Antarctica. Reported drill site conditions – snow accumulation rate, mean annual surface air temperature, ice thickness, and drilling depth – are summarized in Table 1.

The Byrd and Kohnen holes encountered water at the base, which welled up into the holes. The borehole at Vostok penetrated the subglacial Lake Vostok at 3769.3 m, and here, water rose from the lake to a height of more than 340 m. Drilling of other holes was stopped within 10–50 m from the bed. All these holes were temperature logged and provide a good opportunity to fill the gap in our knowledge of the GHF under the Antarctic ice.

https://doi.org/10.5194/tc-2020-32
Preprint. Discussion started: 4 March 2020

2 Methods

2.1 Temperature and temperature gradient at the base of Antarctic Ice Sheet

Temperature in Byrd, WAIS Divide, Vostok, Dome C, Kohnen, and Dome F boreholes were measured using different devices and different methods. All boreholes were mechanically drilled and filled with kerosene-based drilling fluid. Temperature profiles were then obtained by logging with custom-made borehole temperature loggers (Dome C, Kohnen, Dome F, WAIS Divide, and Vostok) or a thermistor embedded into the drill (Byrd).

Temperature measurements in mechanically drilled boreholes filled with drilling fluids are difficult because the increasing temperature with depth can cause convective cell mixing and because of the long time required to get the sensor in equilibrium with the surrounding ice temperature (Clow, 2008). Despite this, we believe that measurement precision in all holes was better than 0.05 °C, and in many instances, did not exceed 0.01 °C. All depth data were recalculated to true vertical depth.

Measured temperature profiles in four of the boreholes (Vostok, Dome C, Kohnen, and Dome F) increase nearly linearly with depth, as would be expected in locations with minimal accumulation and hence small vertical velocities (Fig. 2). Vertical advection is much greater at the Byrd and WAIS Divide boreholes in West Antarctica; in these locations the upper part of the ice sheet is nearly isothermal, but at depth the temperature gradient is nearly the same as at the other sites. Temperature gradients at the bed are 2.02–3.12 °C/100 m at Dome C, Kohnen, Dome F and Vostok and slightly higher in West Antarctica, 3.70–3.88 °C/100 m at Byrd and WAIS Divide (Table 2).

Ice thicknesses generated from extrapolation of temperature profile to the depth of pressure melting point in assumption of Clausius-Clapeyron slope of 0.0742 K/MPa (Cuffey and Paterson, 2010) are in good agreement with radar data, except for the WAIS Divide, where the difference is ~30 m. This could be caused by scintillations on the melted ice-bedrock interface.

2.2 GHF estimation model

A one-dimensional time-dependent energy-balance equation (Dahl-Jensen et al., 2003; Johnsen et al., 1995) is usually used to model the temperature distribution through the ice as a function of the climate conditions on the surface and the GHF from the bedrock:

$$\rho c \frac{\partial T}{\partial t} = \frac{\partial}{\partial z}\left(k \frac{\partial T}{\partial z}\right) - \rho c w \frac{\partial T}{\partial z} - \rho c u \frac{\partial T}{\partial x}, \quad (1)$$

where T is the temperature as a function of z, x and t; z represents the vertical coordinate (at the ice sheet base, z=0, while at ice sheet surface, z=H); H is the ice thickness; x is the horizontal coordinate; t is the time; k is the conductivity of ice dependent on T; ρ is the density of ice; c is the specific heat capacity of ice dependent on T; w and u are respectively the vertical velocity and horizontal velocity of ice sheet dependent on z and t.

We assume that ice sheet is always in thermal steady state and horizontal advection can be neglected (Robin, 1955). This assumption reduces the non-steady-state heat-transfer equation to

https://doi.org/10.5194/tc-2020-32
Preprint. Discussion started: 4 March 2020

$$\frac{\partial}{\partial z}\left(k\frac{\partial T}{\partial z}\right)-\rho cw\frac{\partial T}{\partial z}=0, \quad (2)$$

which can be rewritten as

$$\frac{1}{k}\frac{\partial k}{\partial z}\frac{\partial T}{\partial z}+\frac{\partial^2 T}{\partial z^2}-\frac{\rho c}{k}w\frac{\partial T}{\partial z}=0. \quad (3)$$

Using $\frac{\partial k}{\partial z}=\frac{\partial k}{\partial T}\frac{\partial T}{\partial z}$, the Eq. (3) becomes

$$\frac{\partial^2 T}{\partial z^2}+\left(\frac{1}{k}\frac{\partial k}{\partial T}\frac{\partial T}{\partial z}-\frac{\rho c}{k}w\right)\frac{\partial T}{\partial z}=0. \quad (4)$$

The vertical velocity in the ice is given by (Fischer et al., 2013)

$$w(z)=-w_{melt}-(Acc-w_{melt})\left(\frac{z}{H}\right)^{m+1}, \quad (5)$$

where w_{melt} is the basal melt rate; Acc is the surface accumulation rate dependent on t; m is the form factor that accounts variation of horizontal velocity.

Classically, vertical velocity linearly depends on z/H (Cuffey and Paterson, 2010) and $m=0$. However, at an ice divide, the downward flow of ice is slower, for the same depth, than at locations away from the divide (Raymond, 1983). This reduces the cooling influence of vertical advection and increases the basal temperature. Within this near-divide zone, the form factor could be from 0.5 (Fischer et al., 2013) to 1.0 (Raymond, 1983). All discussed sites are located at, or near, ice divide, thus, we assume m = 1.

Substitution of Eq. (5) into Eq. (4) and integrating on the assumption of k=const gives the following temperature distribution in ice sheet at steady state:

$$T=T_s-\left[\frac{\partial T}{\partial z}\right]_B\int_0^z exp\left(\frac{(w_{melt}-Acc)z^{m+2}}{\alpha_T(m+2)H^{m+1}}-\frac{w_{melt}}{\alpha_T}z\right)dz+\left[\frac{\partial T}{\partial z}\right]_B\int_0^H exp\left(\frac{(w_{melt}-Acc)z^{m+2}}{\alpha_T(m+2)H^{m+1}}-\frac{w_{melt}}{\alpha_T}z\right)dz, \quad (6)$$

where T_s is the surface temperature; $\left[\frac{\partial T}{\partial z}\right]_B$ is the temperature gradient at ice sheet base; $\alpha_T=k/\rho c$ is the thermal diffusivity of ice.

Least square method is used to fit measured borehole temperatures with this equation. In fitting, the initial values of unknown parameters T_s, $\left[\frac{\partial T}{\partial z}\right]_B$, Acc and w_{melt} can only be guessed and this results in unavoidable uncertainty of fitting. To over this large uncertainty, a common genetic algorithm (GA) was designed to find optimal global solution of temperature fitting by limiting these unknown parameters changing in a predetermined range (Reeves and Rowe, 2002). In the GA, the crossover fraction is set to be 0.9 while the migration fraction is 0.2. To obtain accurate solution and save calculation time, we set the population size to be 8000 and the generations to be 20. Usually, after 15 generations of iteration, the optimal solution can be found. All the calculations were performed with MATLAB R2014b software. For each deep borehole, the fitting experiments were trialed five times to avoid random error of GA. Then, the average value in the five fitting experiments was used as the GHF from bedrock into ice at selected site and the uncertainty ranges came from the difference between the maximum/minimum and the average GHF values.

Eq. (4) can also be expressed as

https://doi.org/10.5194/tc-2020-32
Preprint. Discussion started: 4 March 2020


The Cryosphere Discussions

$$w(z) = \left[\alpha_T\left(\frac{\partial^2 T}{\partial z^2}\right) - \alpha_T\left(\frac{1}{k}\frac{\partial k}{\partial T}\right)\left(\frac{\partial T}{\partial z}\right)^2\right] / \frac{\partial T}{\partial z}. \quad (7)$$

Note that the vertical velocity is markedly affected by $\frac{\partial^2 T}{\partial z^2}(z)$ and $\frac{\partial T}{\partial z}(z)$. At the base of the ice sheet, the melt/freezing rate is $w_{melt} = w(0)$, $\left[\frac{\partial T}{\partial z}\right]_B = \frac{\partial T}{\partial z}(0)$. The GHF Q_{geo} from below is balanced by the conductive flux in the ice $q = k\left[\frac{\partial T}{\partial z}\right]_B$ and the energy which is used to melt/freeze ice $J = \rho L w_{melt}$. Thus, the GHF will be:

$$Q_{geo} = \rho L w_{melt} - k\left[\frac{\partial T}{\partial z}\right]_B, \quad (8)$$

where L is the specific latent heat for melting of ice.

3 Results and discussion

Estimations were made for the following ice parameters:

- density 918 kg m^{-3};
- specific heat capacity $c = 152.5 + 7.122\,(T + 273.15)$ J kg^{-1} K^{-1} (Yen, 1981);
- thermal conductivity $k = 9.828e^{-0.0057(T+273.15)}$ W m^{-1} K^{-1} (Yen, 1981);
- specific latent heat L = 333.5 kJ kg^{-1} (Cuffey and Paterson, 2010).

In our model, we assume that k and c are constant and equal to values at the temperature of pressure melting point that can give better estimation of basal melting rate at the base of ice sheet (Fischer et al., 2013). In this case, $\frac{1}{k}\frac{\partial k}{\partial T}$ =-5.7e^{-3} K^{-1}. Estimated vertical velocity profiles are shown on Fig.3. Fig. 4 shows the fitted temperature profiles compared with measured temperatures. Results of our estimates for basal melt/freezing rate and GHF are summarized in Table 2.

The temperature profile shows that the heat flows through the ice at six deep drilling sites in Antarctica must be >42.6–81.4 mW m^{-2} in order to match the observed temperature in the boreholes. The basal ice at all sites is at the pressure-melting point, and the amount of melt cannot be constrained by the energy balance equation alone. When the heat flow model is combined with estimations of vertical velocity, the estimated heat flow can be translated to a GHF of 67.3–251.3 mW m^{-2}, far higher than that predicted by existing heat flow models.

Byrd. Our modeled GHF value at this location (117.8±3.3 mW m^{-2}) is much higher than the first estimation made immediately after temperature logging (75.4 mW m^{-2} referenced by Ueda, 2007) simply because the latter one did not account for the basalt ice melt. The latest modeling (Martos et al., 2017) revealed high GHF at the location of Byrd Station (132 mW m^{-2} with an error of ±5 mW m^{-2}), compared with reference to previous models (An et al., 2015; Fox Maule et al., 2005; Van Liefferinge Pattyn, 2013). This is sufficiently close to our estimations.

Dome C. The inverse approach to retrieving GHF from radar inferred distribution of wet and dry beds at the EPICA drilling site (Passalacqua et al., 2017) gave 54.5±3.5 mW m^{-2}, lower than estimates derived from borehole temperature profiling (67.3±8.6 mW m^{-2}). Modeled GHF range (43–56 mW m^{-2} obtained by An et al., 2015; Fox Maule et al., 2005; Martos et al.,

https://doi.org/10.5194/tc-2020-32
Preprint. Discussion started: 4 March 2020

2017; Shapiro and Ritzwoller, 2004; Van Liefferinge Pattyn, 2013) is also 1.2–1.6 times lower than our estimates. However, a high spatial variation of GHF at Dome C area was found from radar-sounding data (Carter et al., 2009). The values of nearly 100 mW m^{-2} inferred for the southern shore of Concordia Subglacial Lake, approximately 50 km to the south of the drilling site, are also well outside modeled estimates.

Kohnen. The model with a standard GHF of 54.6 mW m^{-2} predicted a basal temperature 0.3 °C below the pressure melting point at Kohnen (Huybrechtset al., 2007). However, subglacial water entering the borehole indicated that the actual GHF should be much higher than that assumed by the standard model. Under these circumstances, our estimates (161.5±10.2 mW m^{-2}) approach to a certain degree the real heat flux.

Dome F. A previously estimated GHF of 59 mW m^{-2} neglected the bottom ice melt rate (Hondoh et al., 2002) and thus is lower than our estimates (79.0±5 mW m^{-2}). As the drill approached the base (approx. 10 m above), subglacial meltwater leaked into the borehole and froze onto the drill, directly indicating that ice reaches the pressure melting point under high GHF.

Vostok. The surface temperature-time curve for the upper bound of the present-day accumulation rate at Vostok corresponds to a GHF of 53 mW m^{-2} (Salamatin et al., 1998). We calculated that at the base of the ice sheet, the conductive flux is 42.6±0.4 mW m^{-2} while the latent heat flux from refreezing of the lake water is 46.3±5.6 mW m^{-2}. Thus, the GHF heat flux at the base of the ice sheet has a negative value of -3.3±5.3 mW m^{-2}. This is in good agreement with the isotope studies that showed that the Vostok ice core consists of ice refrozen from Lake Vostok water, from 3539 m below the surface of the Antarctic ice sheet to its bottom (Jouzel et al., 1999).

At this stage we are not yet able to predict GHF at the bed of 600-m thick subglacial Lake Vostok because temperature profile in the lake is still indefinite. However, the DNA detection of thermophile bacterium in the near-base accretion ice suggests the existence of near-bottom warm waters with temperatures as high as 50 °C (Bulat et al., 2012). If so, the GHF in the lake sediments can reach 200-240 mW m^{-2}. These values can be considered as paleo-GHF because microorganisms were picked up thousands of years ago but still actual accounting for long duration of geological processes.

WAIS Divide. Preliminary estimations of GHF showed quite high values of 215±13 mW m^{-2}, depending on the actual ice thickness (Clow et al., 2012). Our estimates are even higher at 251.3±24.1 mW m^{-2}. The question arises as to whether this high heat flow represents a regional value, or if the WAIS Divide borehole was drilled over a local hot spot. There is no depression in the local surface topography or drawdown in the subsurface layers detected by ice-penetrating radar, as would be expected over a local hot spot. Thus, the high heat flow at this location appears to represent a regional value. How far this heat flow high extends into the interior of the West Antarctic Rift System will require further work.

Prediction of the future behavior of the Antarctic Ice Sheet requires accurate ice-sheet models. However, GHF models based on seismic tomography, radar data, magnetic field observations, the tectonic age and geological structure of the bedrock yielded mixed results at sites of deep ice-core drilling in Antarctica. Processing of available temperature profiles in ice boreholes showed that Antarctica is warmer than predicted. The GHF found at the sites of the EAIS lying on young oceanic crust are 1.1–2.5 times higher than the mean continental GHF. Currently, this phenomenon is also confirmed by tectonic

https://doi.org/10.5194/tc-2020-32
Preprint. Discussion started: 4 March 2020

185 reconstructions (Carson et al., 2014). However, this warm base could be caused by radiogenic or tectonically induced heat effects, and a coherent explanation for this phenomenon is still required. Most numerical models of the EAIS basal conditions assume the GHF to be 42-65 mW m^{-2}. However, the presence of basal meltwater beneath most of the Antarctic ice sheet requires GHF ≥ 80 mW m^{-2} (Budd et al., 1984), which is in good correlation with estimates from the deep drilling sites.

190 Variability of crustal thickness, hydrothermal circulation (Seroussi et al., 2017), magmatic intrusion (Van Wyk De Vries et al., 2017), and thermal conductivity variability are the main contributors to the elevated and highly variable GHF in West Antarctica (Begeman et al., 2017). One of the first pieces of evidence for an "*unreasonably high*" GHF (>100 mW m^{-2}) under WAIS came from temperature-depth profiles in a 480-m-deep borehole drilled at Crary Ice Rise, Antarctica (Bindschadler et al., 1990). The GHF at the vents of subglacial volcanoes in West Antarctica can be as high as 25 W m^{-2} and

195 one such 23-km-wide caldera was revealed ~100 km to the south of the WAIS Divide drill site (Blankenship et al., 1993). However, more precise GHF estimates and explanations for an elevated GHF would be possible after temperature logging and subglacial rocks studies from deep boreholes that are required to drill in Antarctica in the distant future.

Acknowledgments

This work was supported by grant No. 41327804 from the National Natural Science Foundation of China and the

200 Program for Jilin University Science and Technology Innovative Research Team (Fundamental Research Funds for the Central Universities, Project No. 2017TD-24). We are grateful to H. Ueda (retired from USA CRREL) for providing original Byrd borehole temperature-log data. We also thank D. Dahl-Jensen (Centre for Ice and Climate, University of Copenhagen, Denmark) for fruitful discussion and useful comments.

References

205 An, M., Wiens, D.A., Zhao, Y., Feng, M., Nyblade, A., Kanao, M., Li, Y., Maggi, A., and Lévêque, J.-J.: Temperature, lithosphere-asthenosphere boundary, and heat flux beneath the Antarctic Plate inferred from seismic velocities. Journal of Geophysical Research: Solid Earth, 120, 8720–8742, doi:10.1002/2015JB011917, 2015.

Augustin, L., Panichi, S., and Frascati, F.: EPICA Dome C 2 drilling operations: performances, difficulties, results. Ann. Glaciol., 47, 68-72, doi:10.3189/172756407786857767, 2007.

210 Begeman, C.B., Tulaczyk, S.M., and Fisher, A.T.: Spatially variable geothermal heat flux in West Antarctica: Evidence and implications. Geophys Res Lett., 44, 9823–9832, doi:10.1002/2017gl075579, 2017.

Bindschadler, R.A., Roberts, E.P., and Iken, A.: Age of Crary Ice Rise, Antarctica, determined from temperature-depth profiles. Ann Glaciol., 14, 13-16, doi:10.1017/S0260305500008168, 1990.

https://doi.org/10.5194/tc-2020-32
Preprint. Discussion started: 4 March 2020

Blankenship, D.D., Bell, R.E., Hodge, S.M., Brozena, J.M., Behrengt, J.C., and Finn, C.A.: Active volcanism beneath the West Antarctic ice sheet and implications for ice-sheet stability. Nature, 361, 526-529, doi:10.1038/361526a0, 1993.

Budd, W.F., Jenssen, D., and Smith I.N.: A three-dimensional time-dependent model of three West Antarctic ice-sheet. Ann Glaciol., 5, 29–36, doi:10.1017/S026030550000344X, 1984.

Bulat, S.A., Marie, D., and Petit, J.-R.: Prospects for life in the subglacial Lake Vostok. Ice and Snow, 4(120), 92-96, doi:10.15356/2076-6734-2012-4-92-96, 2012.

Carter, S.P., Blankenship, D.D., Young, D.A., and Holt, J.W.: Using radar-sounding data to identify the distribution and sources of subglacial water: application to Dome C, East Antarctica. J Glaciol., 55(194), 1025-1040, doi:10.3189/002214309790794931, 2009.

Carson, C.J., McLaren, S., Roberts, J.L., Boger, S.D., and Blankenship, D.D.: Blankenship, hot rocks in a cold place: High sub-glacial heat flow in East Antarctica. J Geol Soc London, 171(1), 9–12, doi:10.1144/jgs2013-030, 2014.

Clow, G.D.: USGS Polar temperature logging system, description and measurement uncertainties: U.S. Geological Survey Techniques and Methods 2–E3, 2008.

Clow, G., Waddington, E., Hawley, R., and Dahl-Jensen, D.: Subglacial heat flow measurements in Greenland and Antarctica. European Geosciences Union General Assembly, 3-8 April, 2011, Vienna, Austria. Geophysical Research Abstracts 13, abstract id. EGU2011-6629, 2011.

Clow, G.D., Cuffey, K.M., and Waddington, E.D.: High heat-flow beneath the central portion of the West Antarctic Ice Sheet. American Geophysical Union, Fall Meeting 2012, 3-7 December, 2012, San-Francisco, USA, abstract id. C31A-0577, 2012.

Cuffey, K.M. and Paterson, W.S.B. The physics of glaciers, 4th edn. Butterworth-Heinemann, Oxford, 2010.

Davies, J.H.: A global map of solid Earth surface heat flow. Geochemistry, Geophysics and Geosystems, 14, 4608-4622, doi:10.1002/ggge.20271, 2013.

Dahl-Jensen, D., Morgan, V.I., and Elcheikh, A.: Monte Carlo inverse modelling of the Law Dome (Antarctica) temperature profile. Ann. Glaciol., 29, 145-150, doi:10.3189/172756499781821102, 1999.

Dahl-Jensen, D., Gundestrup, N., Gogineni, S.P., and Miller H.: Basal melt at NorthGRIP modeled from borehole, ice-core and radio-echo sounder observations. Ann. Glaciol., 37, 217-212, doi:10.3189/172756403781815492, 2003.

Decker, E.R. and Bucher, G.J.: Geothermal studies in the Ross Island-Dry Valley region. Antarct Geosci, 4, 887–894, 1982.

Ekaykin, A.A., Lipenkov, V.Ya., and Shibaev, Yu.A.: Spatial distribution of the snow accumulation rate along the ice flow lines between Ridge B and Lake Vostok. Lyed i Sneg [Ice and Snow], 4(120), 122-128, doi:10.15356/2076-6734-2012-4-122-128, 2012.

Engelhardt, H.: Ice temperature and high geothermal flux at Siple Dome, West Antarctica, from borehole measurements. J Glaciol., 50(169), 251-256, doi:10.3189/172756504781830105, 2004.

Fischer, H., Severinghaus, J., Brook, E., Wolff, E., Albert, M., Alemany, O., Arthern, R., Bentley, C., Blankenship, D., Chappellaz, J., Creyts, T., Dahl-Jensen, D., Dinn, M., Frezzotti, M., Fujita, S., Gallee, H., Hindmarsh, R., Hudspeth, D.,

https://doi.org/10.5194/tc-2020-32
Preprint. Discussion started: 4 March 2020

Jugie, G., Kawamura, K., Lipenkov, V., Miller, H., Mulvaney, R., Parrenin, F., Pattyn, F., Ritz, C., Schwander, J., Steinhage, D., van Ommen, T., and Wilhelms, F.: Where to find 1.5 million yr old ice for the IPICS "Oldest-Ice" ice core. Clim. Past, 9, 2489–2505, doi:10.5194/cp-9-2489-2013, 2013.

Fisher, A.T., Mankoff, K.D., Tulaczyk, S.M., Tyler, S.W., Foley, N., and the WISSARD Science Team: High geothermal heat flux measured below the West Antarctic Ice Sheet. Sci. Adv., 1(6), e1500093, doi:10.1126/sciadv.1500093, 2015.

Fox Maule, C.F., Purucker, M.E., Olsen, N., and Mosegaard, K.: Heat flux anomalies in Antarctica revealed by satellite magnetic data. Science, 309, 464–467, doi:10.1126/science.1106888, 2005.

Goodge, J.W.: Crustal heat production and estimate of terrestrial heat flow in central East Antarctica, with implications for thermal input to the East Antarctic ice sheet. Cryosphere, 12, 491–504, doi:10.5194/tc-12-491-2018, 2018.

Gow, A.J.: Deep core studies of the accumulation and densification of snow at Byrd Station and Little America V, Antarctica. CRREL Res. Rep. 197, 1968.

Grikurov, G.E. and Leychenkov, G.L.: Tectonic map of Antarctica. CCGM-CGMW, 2012.

Hondoh, T., Shoji, H., Watanabe, O., Salamatin, A.N., and Lipenkov, V.Y.: Depth-age and temperature prediction at dome Fuji station, East Antarctica. Ann. Glaciol. 35, 384–390, doi:10.3189/172756402781817013, 2002.

Huybrechts, P., Rybak, O., Pattyn, F., Ruth, U. and Steinhage D.: Ice thinning, upstream advection, and non-climatic biases for the upper 89% of the EDML ice core from a nested model of the Antarctic ice sheet. Clim. Past, 3, 577–589, 10.5194/cp-3-577-2007, 2007.

Johnsen, S., Dahl-Jensen, D., Dansgaard, W., and Gundestrup N.: Greenland palaeotemperatures derived from GRIP bore hole temperature and ice core isotope profiles. Tellus, 47B, 624-629, doi:10.3402/tellusb.v47i5.16077, 1995.

Jouzel, J., Petit, J.R., Souchez, R., Barkov, N.I., Lipenkov, V.Y., Raynaud, D., Stievenard, M., Vassiliev, N.I., Verbeke, V., and Vimeux F.: More than 200 meters of lake ice above subglacial Lake Vostok, Antarctica. Science, 286(5447), 2138-2141, doi:10.1126/science.286.5447.2138, 1999.

Llubes, M., Lanseau, C., and Rémy, F.: Relations between basal condition, subglacial hydrological networks and geothermal flux in Antarctica. Earth Planet. Sc. Lett. 241, 655–662, doi:10.1016/j.epsl.2005.10.040, 2006.

Lukin, V.V. and Vasiliev, N.I.: Technological aspects of the final phase of drilling borehole 5G and unsealing Vostok Subglacial Lake, East Antarctica. Ann. Glaciol., 55(65), 83-89, 10.3189/2014AoG65A002, 2014.

Martos, Y.M., Catalán, M., Jordan, T.A., Golynsky, A., Golynsky, D., Eagles, G., and Vaughan, D.G.: Heat flux distribution of Antarctica unveiled. Geophys Res Lett., 44, 11417–11426, doi:10.1002/2017GL075609, 2017.

Motoyama, H.: The second deep ice coring project at Dome Fuji, Antarctica. Sci. Drilling, 5, 41-43, doi:10.2204/iodp.sd.5.05.2007, 2007.

Neumann, N., Sandiford, M., and Foden, J.: Regional geochemistry and continental heat flow: implications for the origin of the South Australian heat flow anomaly. Earth Planet. Sci. Lett., 183, 107-120, 10.1016/S0012-821X(00)00268-5, 2000.

Nicholls, K.W. and Paren, J.G.: Extending the Antarctic meteorological record using ice-sheet temperature profiles. J Clim., 6, 141-150, doi:10.1175/1520-0442(1993)006<0141:ETAMRU>2.0.CO;2, 1993.

Parrenin, F., Dreyfus, G., Durand, G., Fujita, S., Gagliardini, O., Gillet, F., Jouzel, J., Kawamura, K., Lhomme, N., Masson-Delmotte, V., Ritz, C., Schwander, J., Shoji, H., Uemura, R., Watanabe, O., and Yoshida, N.: 1-D-ice flow modelling at EPICA Dome C and Dome Fuji, East Antarctica. Clim. Past, 3, 243–259, doi:10.5194/cp-3-243-2007, 2007.

Passalacqua, O., Ritz, C., Parrenin, F., Urbini, S., and Frezzotti, M.: Geothermal flux and basal melt rate in the Dome C region inferred from radar reflectivity and heat modelling. Cryosphere, 11, 2231–2246, doi:10.5194/tc-11-2231-2017, 2017.

Pattyn, F.: Antarctic subglacial conditions inferred from a hybrid ice sheet/ice stream model. Earth Planet. Sci. Lett., 295, 451–461, doi:10.1016/j.epsl.2010.04.025, 2010.

Pittard, M.L., Galton-Fenzi, B.K., Roberts, J.L., and Watson, C.S.: Organization of ice flow by localized regions of elevated geothermal heat flux. Geophys Res Lett., 43, 3342–3350, doi:10.1002/2016GL068436, 2016.

Pollard, D., DeConto, R.M., and Nyblade, A.A.: Sensitivity of Cenozoic Antarctic ice sheet variations to geothermal heat flux. Global Planet. Change, 49, 63–74, doi:10.1016/j.gloplacha.2005.05.003, 2005.

Raymond, C.F.: Deformation in the vicinity of ice divides. J. Glaciol., 29, 357–373, doi:10.1017/S0022143000030288, 1983.

Reeves, C.R. and Rowe, J. E. Genetic Algorithms: Principles and Perspectives. A Guide to GA Theory. Kluwer Academic Publishers, Boston (USA), 2002.

Risk, G.F. and Hochstein, R.: Heat flow at Arrival Heights, Ross Island, Antarctica. New Zeal J Geol Geop., 17, 629–644, doi:10.1080/00288306.1973.10421586, 1974.

Robin, G. de Q.: Ice movement and temperature distribution in glaciers and ice sheets. J. Glaciol., 2, 523–532, doi:10.3189/002214355793702028, 1955.

Salamatin, A.N., Lipenkov, V.Y., Barkov, N.I., Jouzel, J., Petit, J R., and Raynaud, D.: Ice core age dating and paleothermometer calibration based on isotope and temperature profiles from deep boreholes at Vostok Station (East Antarctica). J Geophys Res., 103(D8), 8963–8977, doi:10.1029/97JD02253, 1998.

Seroussi, H., Ivins, E.R., Wiens D.A., and Bondzio J.: Influence of a West Antarctic mantle plume on ice sheet basal conditions. J Geophys. Res. Solid Earth, 122, 7127–7155, doi:10.1002/2017jb014423, 2017.

Shapiro, N.M. and Ritzwoller, M.H.: Inferring surface heat flux distributions guided by a global seismic model: particular application to Antarctica. Earth Planet. Sci. Lett., 223, 213-224, doi:10.1016/j.epsl.2004.04.011, 2004.

Slawny, K.R., Johnson, J.A., Mortensen, N.B., Gibson, C.J., Goetz, J.J., Shturmakov, A.J., Lebar, D.A., and Wendricks, A.W.: Production drilling at WAIS Divide. Ann. Glaciol., 55(68), doi:10.3189/2014AoG68A018, 147-155, 2014.

Ueda, H.T. and Garfield, D.E.: Deep core drilling at Byrd Station, Antarctica. In: A.J. Gow (Ed.) Proceedings of International Symp. on Antarctic Glaciological Exploration (ISAGE), Hanover, New Hampshire, USA, September 3-7, 1968. Association of Scientific Hydrology, Publ. No 86, Cambridge, UK, 53-62, 1970.

Ueltzhöffer, K.J., Bendel, V., Freitag, J., Kipfstuhl, S., Wagenbach, D., Faria, S.H., and Garbe, C.S.: Distribution of air bubbles in the EDML and EDC (Antarctica) ice cores, using a new method of automatic image analysis. J Glaciol., 56(196), 339–348, doi:10.3189/002214310791968511, 2010.

315 Van Wyk De Vries, M., Robert G. Bingham R.G., and Hein A.S.: A new volcanic province: An inventory of subglacial volcanoes in West Antarctica. In: Siegert, M.J., Jamieson, S.S.R., and White, D.A. (eds) Exploration of Subsurface Antarctica: Uncovering Past Changes and Modern Processes. Geological Society, London, Special Publications 461, doi:10.1144/SP461.7, 2017.

Van Liefferinge, B. and Pattyn, F.: Using ice-flow models to evaluate potential sites of million year-old ice in Antarctica.
320 Clim. Past, 9, 2335–2345, doi:10.5194/cpd-9-2859-2013, 2013.

Vasiliev, N.I., Talalay, P.G., and Vostok Deep Ice Core Drilling Parties: Twenty years of drilling the deepest hole in ice. Sci. Drilling, 11, 41-45, doi:10.5194/sd-11-41-2011, 2011.

Wexler, H.: Growth and thermal structure of the deep ice in Byrd Land, Antarctica. J Glaciol., 3(30), 1075-1087, doi:10.1017/S0022143000017482, 1961.

325 WAIS Divide Project Members: Onset of deglacial warming in West Antarctica driven by local orbital forcing. Nature, 500(7463), 440–444, doi: 10.1038/nature12376, 2013.

Wilhelms, F., Miller, H., Gerasimoff, M.D., Drücker, C., Frenzel, A., Fritzsche, D., Grobe, H., Hansen, S.B., Hilmarsson, S.Æ., Hoffmann, G., Hörnby, K., Jaeschke, A., Jakobsdóttir, S.S., Juckschat, P., Karsten, A., Karsten, L., Kaufmann, P.R., Karlin, T., Kohlberg, E., Kleffel, G., Lambrecht, A., Lambrecht, A., Lawer, G., Schärmeli, I., Schmitt, J., Sheldon, S.G.,
330 Takata, M., Trenke, M., Twarloh, B., Valero-Delgado, F., Wilhelms-Dick, D.: The EPICA Dronning Maud Land deep drilling operation. Ann. Glaciol, 55(68), 355-366, doi:10.3189/2014AoG68A189, 2014.

Yen, Y.: Review of thermal properties of snow, ice and see ice. CRREL Rep. 81-10, 1981.

Zagorodnov, V., Nagornov, O., Scambos, T.A., Muto, A., Mosley-Thompson, E., Pettit, E.C., and Tyuflin, S.: Borehole temperatures reveal details of 20th century warming at Bruce Plateau, Antarctic Peninsula. Cryosphere, 6, 675–686,
335 10.5194/tcd-5-3053-2011, 2012.

Zotikov, I.A.: Izmerenie geotermicheskogo potoka tepla v Antarktide [Measurement of the geothermal heat flow in Antarctica]. Sovetskaia antarkticheskaia ekspeditsiia. Informatsionnyi biulleten [Soviet Antarctic Expedition, Information Bulletin] 29, 30–32 [Text in Russian], 1961.

https://doi.org/10.5194/tc-2020-32
Preprint. Discussion started: 4 March 2020

The Cryosphere Discussions
Open Access
EGU

340 **Table 1: Information for Antarctic deep ice-drilling sites**

Parameters	**WAIS**		**EAIS**			
	Byrd	**WAIS Divide**	**Vostok**	**Dome C**	**Kohnen**	**Dome F**
Coordinates	80°01′ S, 119°31′ W	79°28′ S, 112°05′ W	78°28′ S, 106°48′ E	75°06′ S, 123°24′ E	75° S, 0° E	77°19′ S, 39°40′ E
Years drilled	1966-1968[a]	2006-2011[d]	1990–1998, 2005–2014[f,g]	1999-2004[i]	2002-2006[k]	2003-2007[n]
Surface elevation (m a.s.l.)	1530[a]	1766[e]	3488[f]	3233[j]	2892[l]	3810[j]
Drilled depth (m)	2193	3405[d]	3769.3[g]	3270.2[i]	2774.2[k]	3035.2[n]
Ice thickness according with radar/seismic survey (m)	2300[b]	3455[e]	3750±20[g]	3273±5[j]	2750±50[l]	3028±15[j]
Snow accumulation at surface (mm ice a^{-1})	169.5[c]	220[e]	24.8[h]	28.4[j]	70[m]	29.9[j]
Mean surface snow temperature (°C)	-28[a]	-30[e]	-57[h]	-54.6[j]	-44[l]	-57.3[j]

[a]Ueda, 2007; [b]Wexler, 1961; [c]Gow, 1968; [d]Slawny et al., 2014; [e]WAIS Divide Project Members, 2013; [f]Vasiliev et al., 2011; [g]Lukin and Vasiliev, 2014; [h]Ekaykin et al., 2012; [i]Augustin et al., 2007; [j]Parrenin et al., 2007; [k]Wilhelms et al., 2014; [l]Ueltzhöffer et al., 2010; [m]Huybrechts et al., 2007; [n]Motoyama, 2007

https://doi.org/10.5194/tc-2020-32
Preprint. Discussion started: 4 March 2020

345 **Table 2: Thermophysical properties at the base of Antarctic Ice Sheet at sites of deep ice-drilling estimated in this study**

Parameters	WAIS		EAIS			
	Byrd	**WAIS Divide**	**Vostok**	**Dome C**	**Kohnen**	**Dome F**
Temperature, °C	-1.43	-2.30	-2.49	-2.15	-1.85	-1.99
Temperature gradient (°C 100 m^{-1})	3.70	3.88	2.02	2.42	3.12	2.66
Ice thickness according with depth of pressure melting point (m)	2164	3485	3759	3257	2770	3016
Basal melt rate (mm a^{-1})	4.2±0.3	17.5±2.3	-4.8±0.6	1.7±0.8	9.9±1	2.5±0.5
GHF (mW m^{-2})	117.8±3.3	251.3±24.1	-3.3±5.6	67.3±8.6	161.5±10.2	79.0±5.0

https://doi.org/10.5194/tc-2020-32
Preprint. Discussion started: 4 March 2020

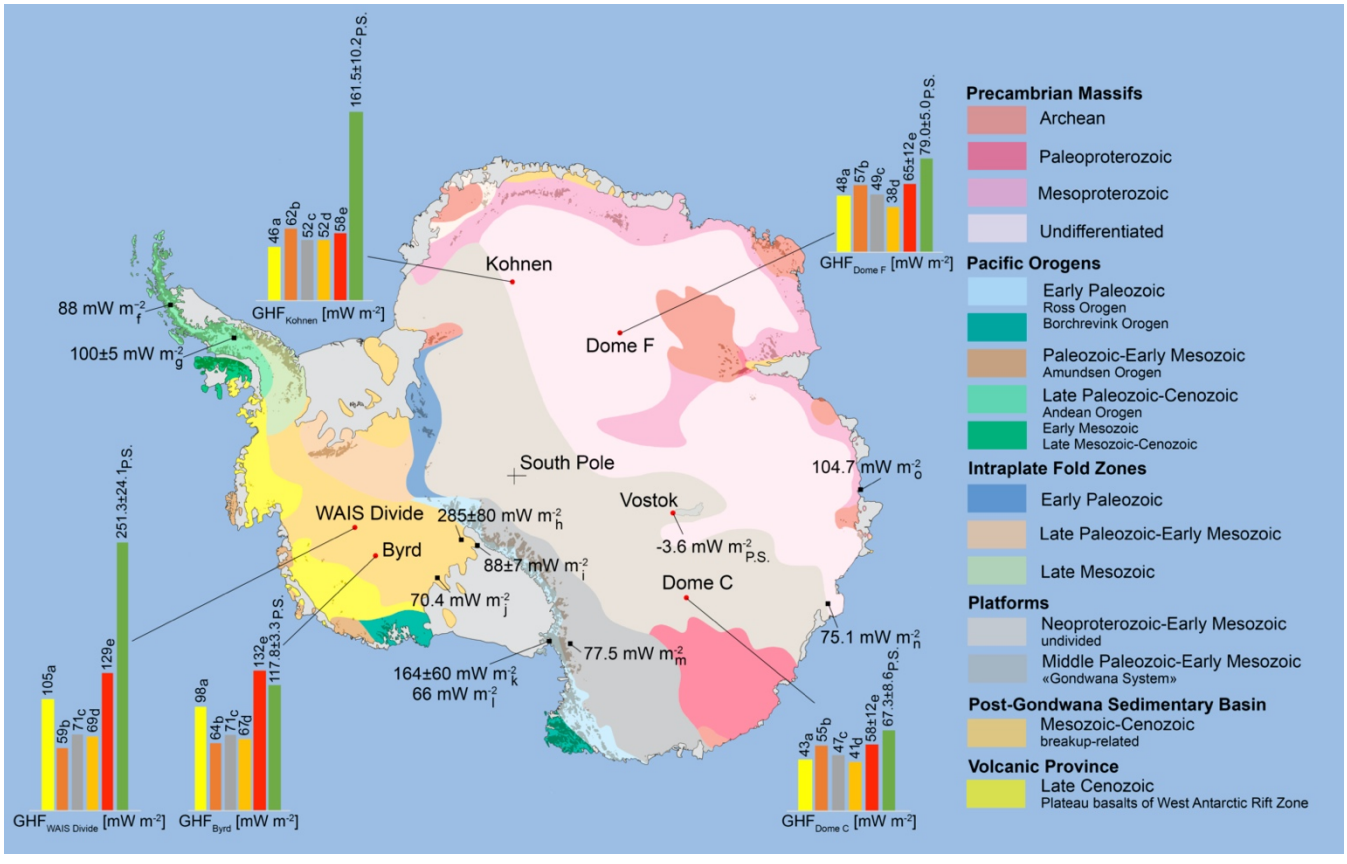

Figure 1: GHF derived from basal temperature gradients in deep ice boreholes (green bars) compared with modelling ([a]Shapiro and Ritzwoller, 2004; [b]Fox Maule et al., 2005 [c]Van Liefferinge and Pattyn, 2013; [d]An et al., 2015; [e]Martos et al., 2017). Red circles show locations of deep ice drilling sites (Byrd, WAIS Divide, Vostok, Dome C, Kohnen, and Dome F) discussed in the present study (P.S.). Black squares show locations of boreholes drilled in Antarctic margins, in which borehole temperature measurements were carried out and GHF values were estimated ([f]Zagorodnov et al., 2012; [g]Nicholls and Paren, 1993; [h]Fisher et al., 2015; [i]Begeman et al., 2017; [j]Engelhardt, 2004; [k]Risk and Hochstein, 1974; [l]Decker and Bucher, 1982; [m]Clow et al., 2011; [n]Dahl-Jensen et al., 1999; [o]Zotikov, 1961). Drill sites in ocean/sub-shelf sedimentaries are not shown. A simplified tectonic map (Grikurov and Leychenkov, 2012) is used as the background.

https://doi.org/10.5194/tc-2020-32
Preprint. Discussion started: 4 March 2020

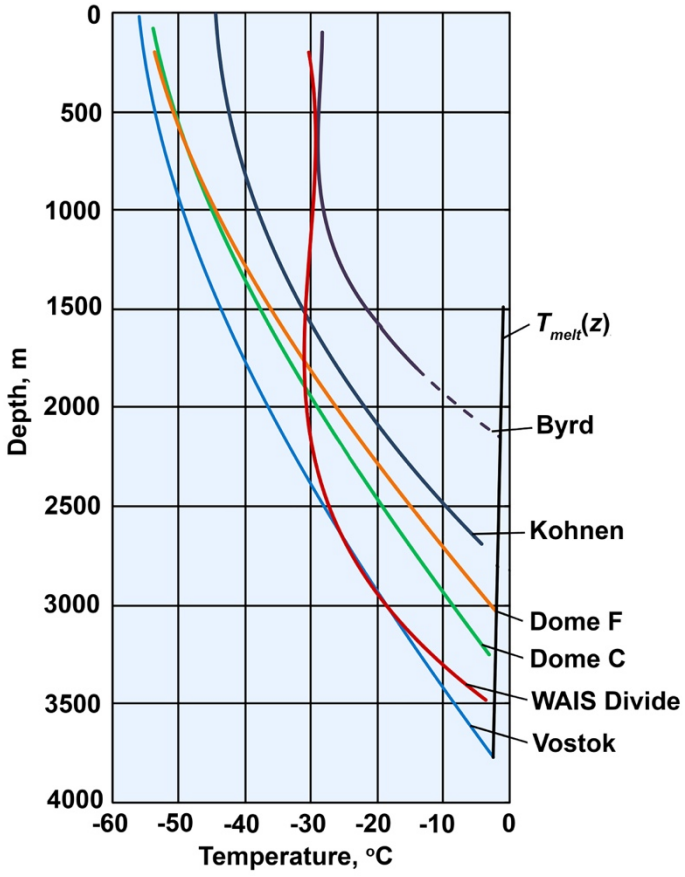

Figure 2: Smoothed measured temperature profiles in Antarctic deep ice boreholes. Pressure-melting point temperature $T_{melt}(z)$ is shown in the assumption of Clausius-Clapeyron slope of 0.0742 K/MPa.

360

https://doi.org/10.5194/tc-2020-32
Preprint. Discussion started: 4 March 2020

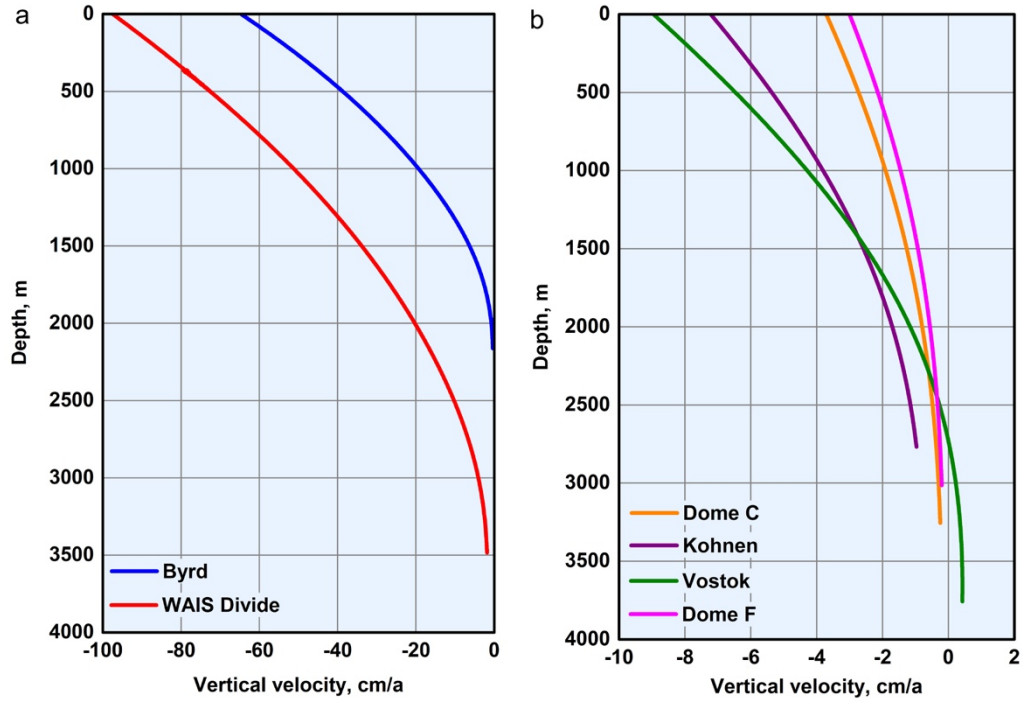

Figure 3. Estimated vertical velocities at drilling sites in West Antarctica (a) and East Antarctica (b). In East Antarctica snow accumulation and thus vertical ice velocities are far less than in West Antarctica.

365

https://doi.org/10.5194/tc-2020-32
Preprint. Discussion started: 4 March 2020

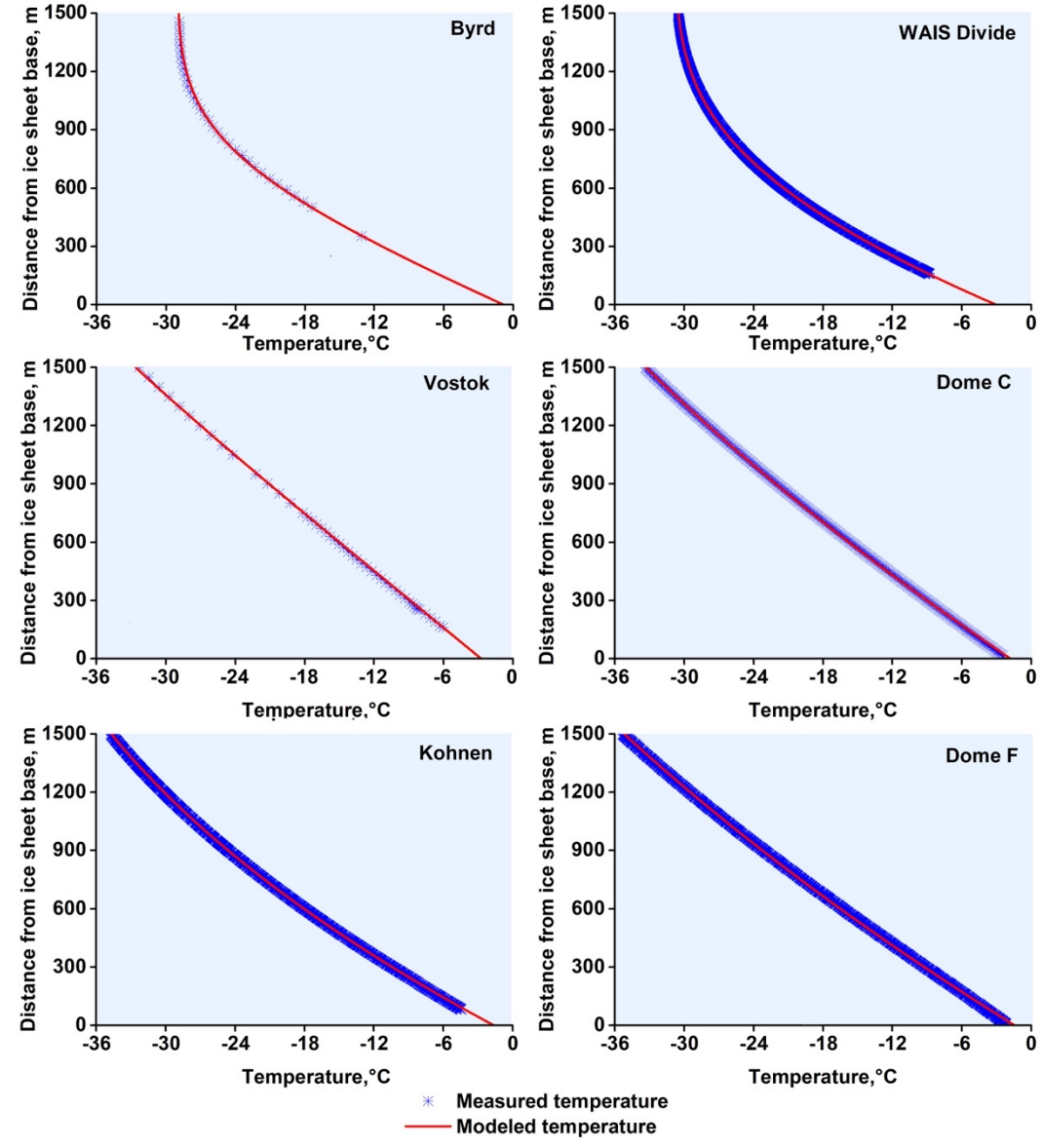

Figure 4. Temperatures measured in Antarctic deep ice boreholes compared with best-fit temperature profiles for the deepest 1500 m.